

# Growth of polymer microstructures between stressed silica grains: a chemo-mechanical coupling

R. GUO\* and T. HUECKEL\*

Laboratory tests on the micro scale are reported in which two amorphous silica cubes were compressed in a liquid environment, in solutions with different silica ion concentrations, for up to three weeks. Such an arrangement represents an idealised representation of two sand grains. The grain surfaces and asperities were examined in the scanning electron microscope and atomic force microscope (AFM) for fractures, silica gel growth, and polymer strength. In 500 ppm solution, silica gel structures a few hundred micrometres long appeared between stressed silica cubes. In 200 ppm solution, silica deposits were found around damaged grain surfaces, while at 90 ppm (below silica solubility in neutral pH), fibres a few micrometres in length were found growing in cube cracks. AFM pulling tests found polymers with strength of the order of 100 nN. We concluded that prolonged compression produced damage in grains, raising local silicon ion concentration, and accelerating precipitation, polymerisation and gelation of silica on grain surfaces, enhancing soil strength at the micro scale, and hence most likely contributing to the ageing phenomenon observed at the macro scale.

KEYWORDS: chemical properties; particle-scale behaviour; sands; stiffness; time dependence

## INTRODUCTION

Soils exhibit significant stiffening when subjected to prolonged compression at a constant load – what is known under the name of soil ageing (Mitchell & Solymar, 1984; Hueckel *et al.*, 2005).

Soil ageing occurring in silts, sands, and sand–clay mixtures at the engineering timescale (hours, weeks, or months; Joshi *et al.*, 1995; Hueckel *et al.*, 2001, 2005; Bowman & Soga, 2003) bears many common features with pressure solution phenomenon during diagenesis. Diagenesis is of interest in geochemistry, structural geology and petroleum engineering, and is believed traditionally to occur over geological times (Sorby, 1862; Rutter, 1976). Notably, the focus in pressure solution studies is on mineral mass transfer and on porosity and permeability evolution, rather than stiffening of the medium. In both phenomena, creep is seen as a main component of the process.

While the phenomenon has been extensively measured in the field and in the laboratory experiments, the mechanisms behind soil ageing and variables controlling it remain a subject of intense research (Baxter & Mitchell, 2004). Ageing in dry clean sand is attributed to creep or secondary consolidation of sand. It is suggested that particles continuously rearrange until stable equilibrium positions are reached under applied load and kinematic constraints (Mesri *et al.*, 1990; Schmertmann, 1991; Bowman & Soga, 2003; Wang *et al.*, 2008). The presence of fines in dry sand soils also increases creep strain and ageing rate (Wang & Tsui, 2009). The mechanical properties of granular assemblies at the macroscopic level are known to be affected by contact networks, on the one hand, and the local response of grain contact neighbourhoods on the other (Parry, 2004). In the latter case, the response is determined not only by the

material itself, but also by how the grains of the material interact with each other under stress. The physical (or chemical) driving processes behind particle system rearrangement under constant load and their rates are not well known, and are hypothesised to be mostly local, interparticle processes: time-dependent interparticle friction, plastic yielding of grain asperities following a chemical reaction rate law (Eyring, 1936; Kuhn & Mitchell, 1993), capillary condensation of atmospheric moisture (Paterson & Kekulawala, 1979; Israelachvili, 2011), and plastic or visco-plastic microcracking due to indentation in the contact area (Scholz & Engelder, 1976; Tada *et al.*, 1987; Hickman & Evans, 1995; Hu & Hueckel, 2007a). However, the links between such microscopic and localised processes and possibly ensuing reconfiguration of particle chains, and then the strengthening of soil at a macro scale, while very likely, are far from being proven, as stressed by Kuhn & Mitchell (1993).

Still efforts using numerical tools to show that such hypothetical micro-scale mechanisms are consistent with the upscaled macroscopic behaviour of soils (e.g. Kuhn & Mitchell, 1993; Hu & Hueckel, 2007a).

In saturated conditions, sand exhibited a 200% (with seawater) to 220% (with distilled water) larger penetration resistance after 1 year of ageing compared with 30% larger penetration in dry conditions (Joshi *et al.*, 1995). Cohesion was also significantly larger in sand when submerged in water under constant load, compared with the same sand in dried conditions. Joshi *et al.* indicated the presence of cement bonding between grains due to dissolution and precipitation of salts, and possibly silica, as the source of the difference. Hence the mechanisms of ageing in the wet condition are not purely mechanical, but are coupled with much more significant chemical processes, such as dissolution, precipitation, and possibly polymerisation and gelation of materials around the contact region (Hu & Hueckel, 2007a, 2007b). Therefore there is sufficient evidence to claim that strain and stress alone cannot alter the mechanical properties of granular materials over time to the level that they do in the presence of pore fluid. It is not known at present what the specific mechanisms of coupling are

Manuscript received 4 March 2012; revised manuscript accepted 23 October 2012.

Discussion on this paper is welcomed by the editor.

\* Department of Civil and Environmental Engineering, Duke University, Durham, NC, USA.

between the chemical process and grain structure rearrangement, to produce such a significant overall change in the mechanical properties of soil.

In nature, the processes of dissolution and redistribution of mass in tight rocks takes time on the geological scale, such as during the formation of sandstone by the amorphous silica mass that binds the sand grains together (Worden & Morad, 2000). However, experiments at both the macro scale and the micro scale have shown that such processes can also occur on a timescale of days, weeks, or months (Denisov & Reltov, 1961; Hueckel *et al.*, 2001, 2005; Meyer *et al.*, 2006; Hu & Hueckel, 2007b). Interestingly, in terms of compressibility decline monitored over 3 months, up to 85% of the change occurs in the first two weeks of the process (Hueckel *et al.*, 2001). A similar conclusion in terms of mass transfer was reached by Oelkers *et al.* (2008).

One of the earliest hypotheses explaining the changes in the strength of sand was put forward by Denisov & Reltov (1961), who conducted experiments indicating that the strength of the compacted submerged granular medium increases gradually, owing to the formation of silicic acid gel at the quartz surfaces in contact. On the other hand, in studies of pressure solution it was noticed that the presence of clay in the vicinity of contact substantially enhances the dissolution of quartz (Becker, 1995; Bjorkum, 1996; Kristiansen *et al.*, 2011). Much more recently, atomic force microscopy (AFM) and scanning electron microscopy (SEM) studies of the stressed silica–muscovite contact have indeed shown a silica dissolution rate almost an order of magnitude higher at room temperature and low pressure to maintain contact. This has previously been observed in sandstones in the presence of mica (Heald, 1955; Renard *et al.*, 1997). It is believed that the enhanced silica dissolution has a much higher rate, and is due to the difference in surface electrochemical potentials (Meyer *et al.*, 2006). Meyer *et al.* (2006) also revealed the development of silica gel structures in the vicinity of the stressed contact.

The present work aims at clarifying the role and conditions of formation of polymeric silica structures between synthetic silica grains, as suggested originally by Denisov & Reltov (1961), and endorsed by numerous subsequent studies. In previous work (Hu & Hueckel, 2007a) the authors have theorised a mechanism through which a granular material stiffens in submerged stressed conditions. It is the generation of microcracking near the stressed intergranular contact that constitutes a source of an increasing specific surface area of interphase interface at which dissolution of quartz occurs. This dissolution removes the mineral from the solid phase, making the material in that zone weaker, and further enhancing the process of microcracking (Hueckel *et al.*, 2001). The dissolved mineral may either migrate away in the presence of advective gradients or, in their absence, when local concentrations grow sufficiently, precipitate, polymerise or gelate. Driven by these hypotheses, the grains will be brought in contact to stress conditions that are slightly below the onset of microcracks, and the system will be kept closed to any dissolved silica transport.

Specifically, this study presents preliminary findings from a set of experiments on the effect of the polymerisation of silica in the intergranular space on the bonding of one quartz grain asperity and another quartz grain during environmentally mediated indentation. The experiments included: precipitation and quantifications of silica polymerising on unstressed quartz grains; the AFM tensile strength of individual silica polymer chains; the enhancement of silica polymerisation due to stressing and damage of indenting grains; the tensile strength of intergranular silica gel bonds; the effect of the presence of muscovite mica sheet, and a lowered pH of the fluid, on gelation, polymerisation and structure formation.

The study focuses on short-timescale phenomena (two to three weeks), seen to produce sufficient dissolution and precipitation, as well as compressibility change (Hueckel *et al.*, 2001, 2005; Meyer *et al.*, 2006; Kristiansen *et al.*, 2011). Laboratory experiments are presented where amorphous silica grains were compressed in a liquid environment rich in Si ions for up to three weeks. Silica deposits and polymers observed in the stressed contact region using SEM and AFM are measured and tested mechanically.

## MATERIALS AND METHODS

### *Silica cubes and silicic acid*

The quartz grains in stressed contact were simulated using amorphous silica cubes (Figs 1(a) and 1(b)). Silica is found in both crystalline and amorphous forms in nature. Crystalline silica has long-range orders, involving a tetrahedral coordination of four oxygen atoms around a silica atom. Quartz is by far the most common crystalline form of silica, found in natural sand (Iler, 1955). Amorphous silica, on the other hand, does not have any long-range order, but a tetrahedral arrangement between oxygen and silica atoms still exists locally. The choice of amorphous silica for the test was motivated by two substantial considerations. First, the rate of dissolution of amorphous silica is about one order of magnitude greater than that of its crystalline counterpart (Iler, 1955). It appears that this would not only reduce the time of the tests, but also would lower the risk of biological contamination. Second, most quartz grains in nature, which are predominantly crystalline, are enveloped by a layer of amorphous quartz (Oelkers *et al.*, 1992). It is believed that such an envelope is generated by silica dissolved from the rock in the presence of mica (muscovite). Hence, for two grains in contact, the indentation of an asperity would penetrate first through the amorphous coating.

The silica cubes used are made of unpolished amorphous quartz (Prism Research Glass Inc.). Quartz sheets are either laser-cut into 1.5 mm × 1.5 mm × 1 mm parallelepipeds, or blade-cut in to 30 mm × 30 mm × 30 mm cubes to simulate common natural sand grain size. The laser processing of cubes has the disadvantage of producing edges that are relatively round, and of irregular length and inclination. This reduced the effectiveness of such edges as indenters.

The indenting amorphous quartz cubes are placed in a liquid environment containing an already high concentration

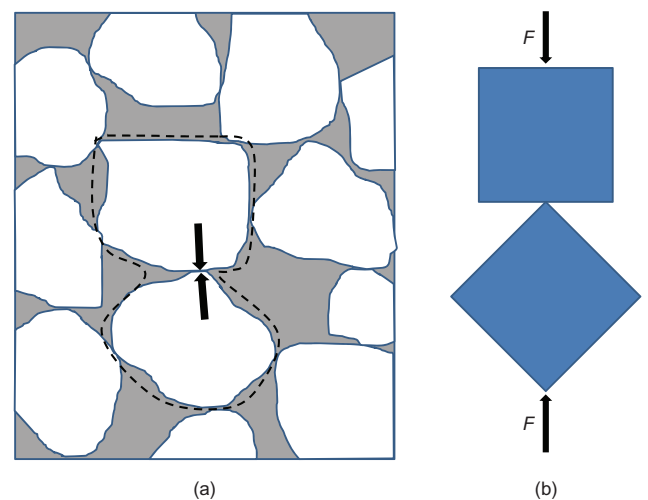


**Fig. 1. Configurations of compressed cubes in nature and in laboratory setting to simulate intergranular stress: (a) 2D representation of granular material; (b) laboratory simulation of two grains in stressed contact in dotted line in (a)**

of silica to accelerate precipitation. To prepare the solution to be used in the liquid chamber, silicic acid powder ( $\text{H}_2\text{SiO}_3$ ; Fisher Scientific) was added to 5 M NaOH solution for complete ionisation. Solutions with different Si ion concentrations can then be made by diluting this solution with nano-pure water. The pH value of the solution remained above 10.0 to prevent the Si ions from precipitating and polymerising. Immediately before each experiment, 1 M nitric acid was used to lower the pH value of the solution to between 5.0 and 5.5, to simulate natural water. No glass containers were used during the experiment, to prevent extra Si ions from glass dissolving in the solutions.

#### Quartz cube indenter

To simulate soil grains in compression, a quartz cube environmental indenter as constructed at Duke University by C. J. Rubin (Rubin, 2009) was used (Fig. 2). The central part of the apparatus is the sample holder, where one silica cube is placed on a platform in the liquid chamber at a  $45^\circ$  angle in such a way that its corner edge faces the side of the other cube held in a pincer. The liquid chamber is made of stainless steel, and is connected to a pneumatic actuator (Bimba TB-1625) by a rod, also made of stainless steel. The rod passes through an O-ring, which prevents leakage around the rod. A small pincer is screwed onto the rod in the liquid chamber, allowing the mobile silica cube to be indented with a monitored displacement into the other cube. The indentation force is recorded.

After placing two silica cubes in their respective positions, the actuator is activated, which pushes the rod forwards and press one silica cube at the end of the rod against the other cube on the platform in the liquid chamber. The pressure in the pneumatic actuator is then gradually increased to 170 kPa to prevent sudden movement of the rod crushing the cubes. A solution containing Si ions is immediately added to the liquid chamber, and the chamber is sealed off by Parafilm and left to mature under constant force for up to three weeks using a pressure controller (Norgren Excelon Pro). Details of the indenter design and characteristics can be found in Rubin (2009). Images of the contact region between cubes before and after the experiment were taken using SEM (FEI XL30 ESEM) for comparison.

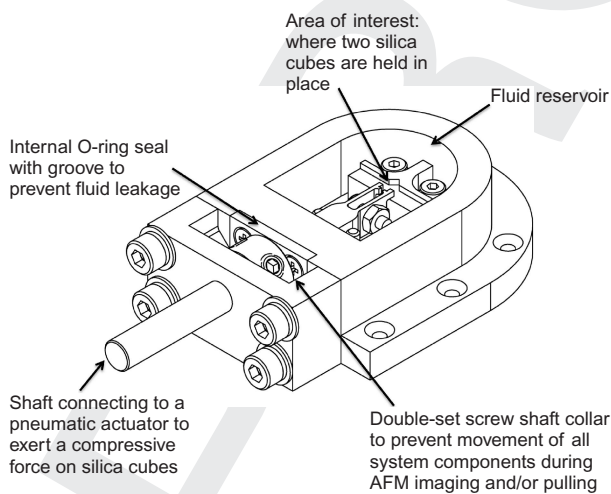


**Fig. 2.** Central part of pneumatic cube indentation device. Left cube sits on platform with edge pointing to the right. Right cube secured by a pincer and pushed to the left by shaft connected to pneumatic actuator (not shown). Double-set screw collar on the right prevents shaft movement during AFM imaging and/or pulling

#### Silica polymer strength

In another experiment, designed to measure the mechanical strength of silica micropolymer chains, an amorphous silica cube was placed in solution with a predetermined Si ion concentration for three weeks. A liquid pulling experiment was conducted on the cube surface using AFM (Digital Instruments Dimension 3100) and Veeco TESP k cantilevers. The cantilever tip was repeatedly lowered onto the cube surface with silica polymers on it and then raised. If the tip has picked up a silica-polymer-linked backbone on the cube surface, raising it would straighten the polymer and cause the cantilever to bend until the polymer chain broke. The force required to break the silica polymer chain can be calculated using the recorded cantilever tip deflection and tip spring constant.

#### Silica gel growth in solution

Since solutions prepared for most of the cube compression experiments were supersaturated in silica, it is necessary to find the undisturbed precipitation and polymerisation rate of silica and determine the extent to which the supersaturation of silica contributes to the growth of polymers and deposits found around stressed contact regions. Part of the same solution with 300 ppm Si ion concentration that was used to fill the liquid chamber for cube compression experiments was stored in petri dishes and allowed to mature for silica gel growth in an undisturbed environment. Samples from the solutions were examined by AFM fluid imaging in tapping mode at various stages over three weeks to determine the size and growth rate of the silica gels.

#### Silica cube indenter-puller

An indenter-puller device was built in order to measure the tensile strength of the intergranular silica polymer (Fig. 3). The two cubes are pushed together with a layer of  $10\ \mu\text{m}$  mica sheet between. The force applied can be calculated by multiplying the springs' compression length with their spring constants. The spring compression can be changed by turning the four wing-nuts on the top plate. The cubes are submerged in a liquid bath with a predetermined Si ion concentration. The whole device is then sealed in a Styro-foam box together with a wetted sponge to minimise water evaporation. A ring is inserted on the bottom plate around the cubes to create a semi-enclosed environment to help

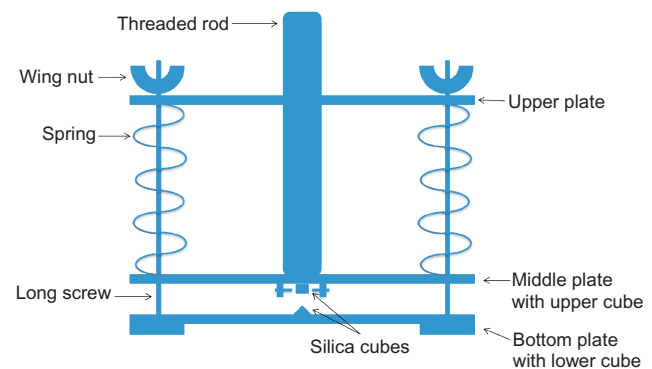


**Fig. 3.** Schematic of cube indenter-puller. One cube sits on bottom plate with one edge pointing upwards. Other cube clamped on middle plate by screws with flat face facing downwards. Four long screws through all three plates keep them together. Springs compressed by turning wing nuts on top plate. Long threaded rod connects middle plate to load frame during extension experiment

retain dissolved silica ions in the vicinity of the contact region. The plates and the ring are made of aluminium, and all other screws are made of stainless steel.

After 10–20 days, the device is taken out of the Styro-foam box and connected to a load frame (Tinius Olsen H50K-S) by a long threaded rod and lowered onto an analytic scale (Mettler Toledo AL204) until the reading on the scale slightly exceeds the total weight of the bottom plate and the lower cube, measured before the experiment. The upper plate, springs and screws are then removed from the device, while the cubes on the lower and middle plates are still sitting on the scale and pressed together. The load frame is then raised at a speed of 0.050 mm/min until the two cubes are completely detached from each other. The reading on the scale is captured by a video camera. Immediately before the two cubes separate, any intergranular silica polymers grown between the two cubes are stretched, and an uplifting force is created on the lower cube. Such an uplifting force lowers the reading on the analytical scale momentarily until all polymer contacts are broken and the weight on the scale returns to a constant. The intergranular mechanical force is calculated by taking the difference in mass reading recorded by the analytical scale.

Two experiments were conducted, one using a solution with 500 ppm Si ion concentration and aged for 10 days; and the other a solution with 300 ppm Si ion concentration and aged for 20 days. In both experiments the compression force applied to the cubes was 180 N.

#### *Experiments in the presence of muscovite*

To investigate the effect that muscovite has on the dissolution, precipitation and polymerisation of silica around the contact region, the cube indentation experiment mentioned 2 is repeated with a 10  $\mu\text{m}$  highest-grade muscovite mica sheet (S&J Trading, New York) inserted between the two quartz cubes. The cubes were under 140 kPa pressure for 2 weeks in a solution with 300 ppm Si ion concentration. SEM images of the contact region are taken at the end of the experiment.

## RESULTS

### *Silica cubes compressed in solutions containing Si ions*

A series of tests to assess the rate of production of silica polymer were conducted at different elevated concentrations of silica ions in the environmental solution. The rationale for using an initial elevated concentration (Rubin, 2009), after finding a concentration high enough to induce polymerisation or gelation, is to bring the concentration somewhat below that level, and allow some time for sufficient dissolution from the damaged material to bring the solution to the level at which silica will polymerise. (The concentration of silica in the pore solution may be much higher locally and instantaneously near the asperities and stressed and dissolving contacts than the average pore water concentration.)

*In 500 ppm Si ion concentration solution.* After two silica cubes were pressed against each other for 3 weeks in solution with 500 ppm Si ion concentration, polymers were observed on the surfaces of both cubes in the SEM (Fig. 4). Some of the polymers connected to both cubes near the contact regions were up to several hundred micrometres long. A composition analysis of such polymers using an energy dispersive X-ray spectrometer (EDS) on the SEM showed that the structures were mostly silica, with minor traces of Cl, Cr, Fe, Na and C elements (Fig. 5). The minimal amount of carbon in the sample may come from dust in the

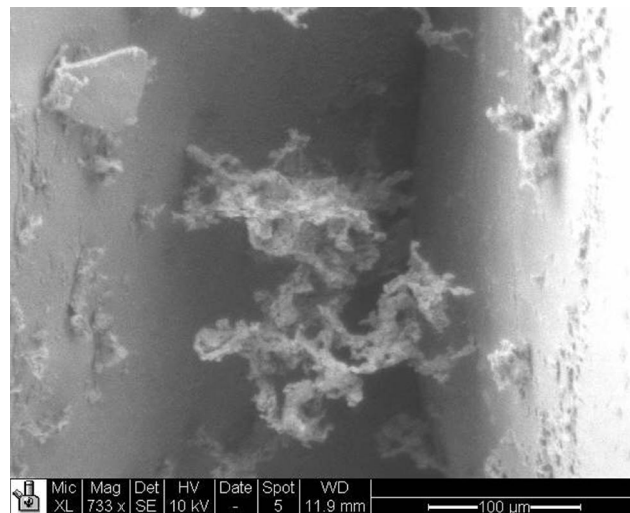


**Fig. 4.** SEM image of silica polymers growing around stressed contact region between two silica cubes after 3 weeks in solution with 500 ppm Si ion concentration and neutral pH

environment, and shows that the structure is not of biological origin, otherwise carbon would be a dominant element in the polymer structure.

*In 300 ppm Si ion concentration solution.* A similar experiment with the same set-up, but using 300 ppm Si ion concentration solution for 2 weeks, showed extensive silica deposits with size of the order of 10  $\mu\text{m}$  developed near the asperities as a result of compression (Fig. 6(a)). The experiment was repeated with a lower pressure (120 kPa) applied to the cubes from the pneumatic actuator. It was found that no microcracks had developed on either cube, and no silica polymer deposits were found anywhere in the liquid chamber (Fig. 6(b)).

*In 90 ppm Si ion concentration solution.* Polymers a few micrometres in length were found between a cube's main body and a piece of silica debris that was chipped off by compression (Fig. 7). No extensive silica deposits were found otherwise.

Comparing the size of these silica deposits with that of silica polymers found growing in solution with the same Si ion concentration, but without compressed silica cubes in the solution, the rate of silica gel growth around the stressed contact was found to be greater than in the undisturbed solution.

### *AFM pulling experiments on silica cube surfaces*

Undisturbed (not loaded) silica cubes left in solutions with Si ion concentrations ranging between 130 ppm and 210 ppm for 2 weeks were put in the AFM, and pulling experiments in water were conducted on the cube surfaces. On the surfaces of the cube that was in the 210 ppm solution, distinctive kinks were consistently captured on the force curves (Figs 8(a) and 8(b)). The blue curve represents the force curve as the cantilever tip approaches the surface. The red curve represents the force curve as the cantilever pulls away from the surface. The vertical distance between the two curves can be converted to the additional force required for the cantilever to overcome surface tension, short-range forces, and any potential polymers connecting the tip to the surface, by multiplying the cantilever deflec-

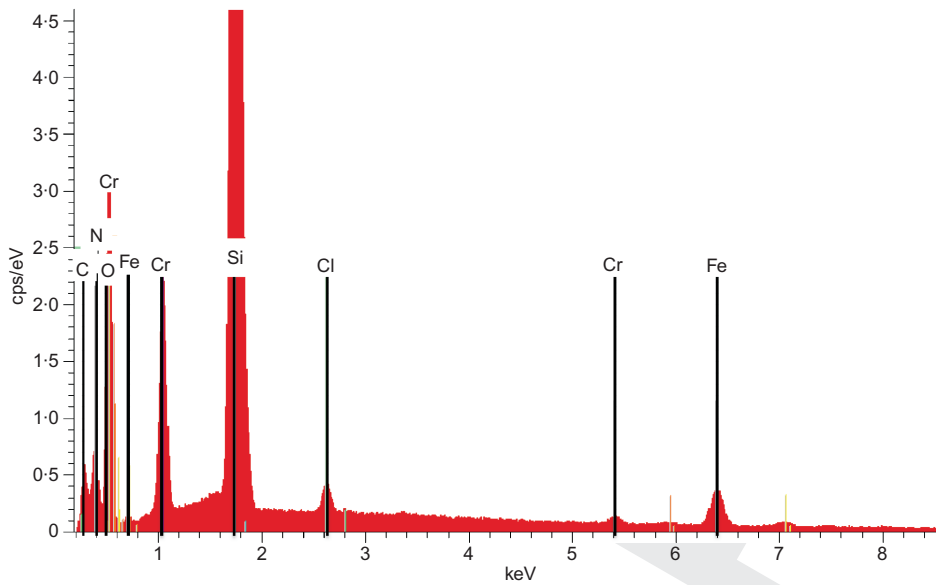
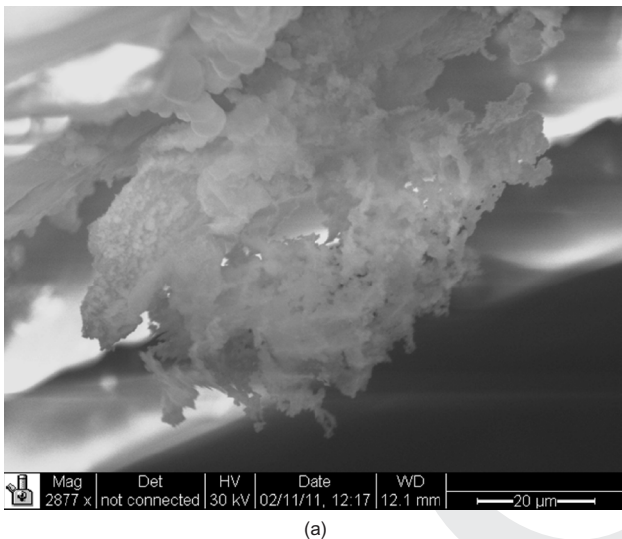


**Fig. 5. EDS spectrometer analysis of polymer chemical compositions. Silica the dominant element; other elements include chromium, iron, chloride, sodium, oxygen and carbon**



(a)

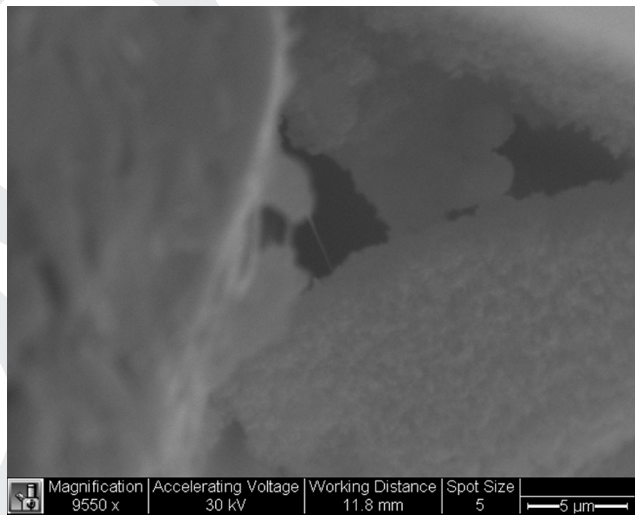
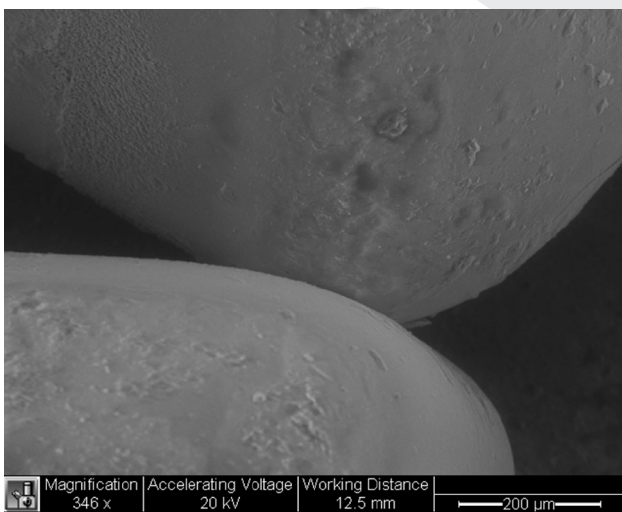


**Fig. 7. SEM image of two silica polymers less than 5 μm long growing between silica cube main body and piece of silica debris at centre of image**



(b)

**Fig. 6. SEM images of contact regions between silica cubes in 300 ppm Si ion concentration solution for 3 weeks: (a) silica deposits growing in cube cracks when cubes under 170 kPa pressure; (b) clean cube surfaces with no microcracks and no silica deposits when cubes under 120 kPa pressure**

tion sensitivity (30 nm/mV) and the spring constant (0.74 nN/nm). The peaks shown in Figs 8(a) and 8(b) may represent instances when polymer segments were broken as the cantilever was pulling away, and therefore the vertical distances between the peaks of the two curves can be converted to force magnitude for an estimation of polymer strength. In Fig. 8(a) the average vertical distance from a peak is about 15 mV, which converts to about 330 nN, whereas in Fig. 8(b) the average peak distance is 21 mV, equivalent to about 450 nN force. Such force patterns were not obtained on cube surfaces in solutions with 130 ppm and 170 ppm Si ion concentrations. Small jumps were recorded when the tip was about to leave the cube surfaces, but they most probably occurred as a result of surface tension.

#### *Growth of silica gels in undisturbed supersaturated solution*

Samples of 300 ppm silica ion concentration solution were taken from a sealed plastic test tube 1 week and 2 weeks after the experiment started at day 0, and imaged in AFM

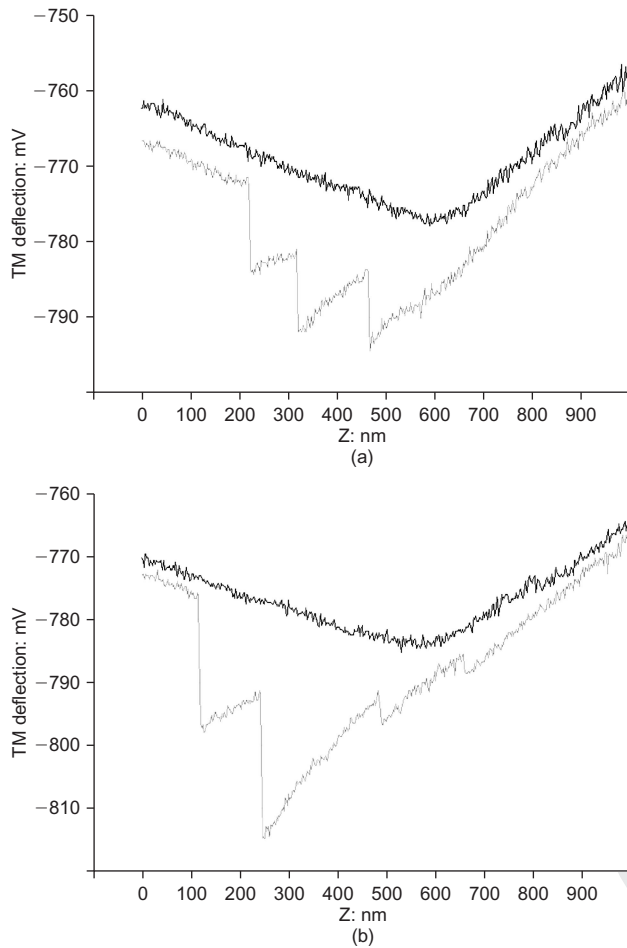


**Fig. 8.** AFM force curves of silica polymers growing on cube surface in solution with 210 ppm Si ion concentration and neutral pH

fluid imaging mode. To maintain the concentration of silica ions in the solution, the test tube was filled fully to minimise the air space between the liquid surface and lid in order to minimise evaporation. Figs 9(a) and 9(b) show the growth of silica structures at day 8 and day 15 respectively. At day 8 (Fig. 9(a)), many silica seeds with diameter of the order of 10s of nanometres appear in the solution, represented as bright spots on the mica substrate; at day 15 (Fig. 9b), an interconnected network of gel appears in the solution, but the height of the structure was only around 30 nm, and each polymer width was at least one magnitude less than 1  $\mu\text{m}$ . Nevertheless, the density of such structures and their interconnectivity is quite impressive.

#### *Silica cube environmental compression with damage followed by an extension test*

The test made it possible to calculate the resultant force at rupture of the entire gel, as follows. The scale measures the mass of the bottom plate and cube, minus an uplifting intergranular force between the top and bottom cube. The minimum reading of the scale during cube separation represents the value at the onset of the decrease of the intergranular force. Hence the difference between that reading and the final reading after two cubes are well separated represents the maximum intergranular force. To isolate the capillary force between the cubes from this result, a control experiment was performed in which clean silica cubes and mica sheet were compressed and immediately separated. The force value from the control experiment is taken off from

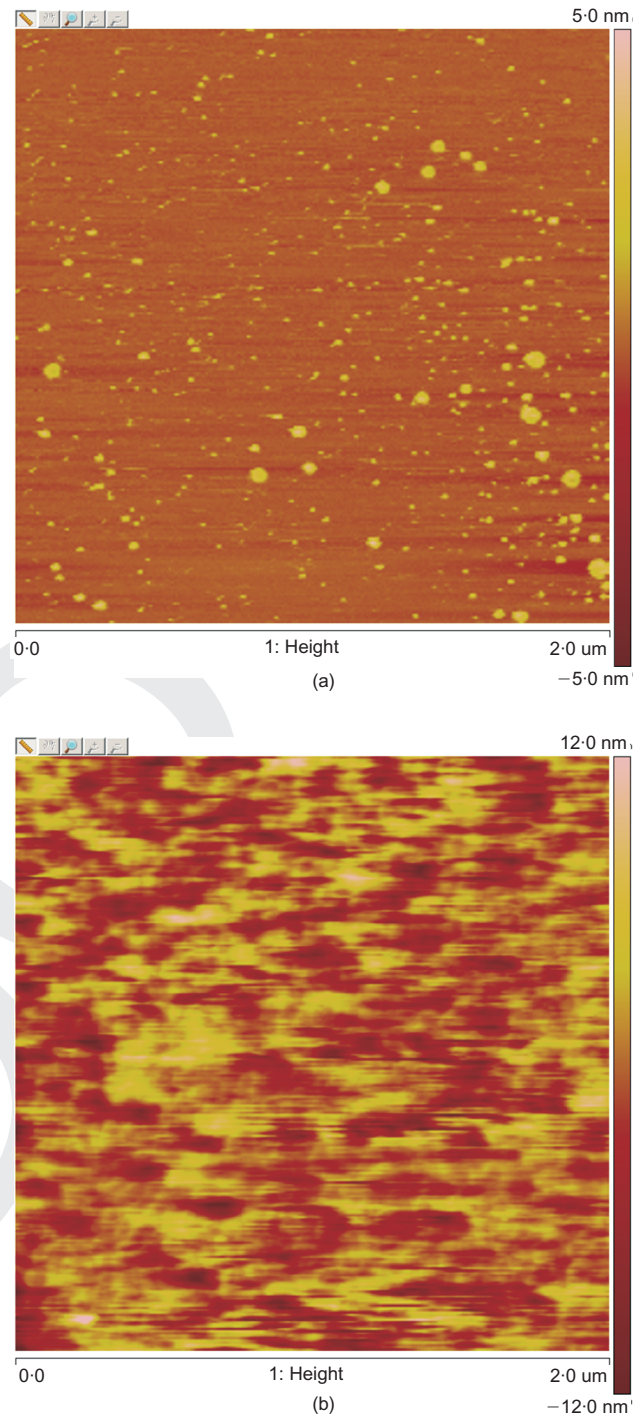


**Fig. 9.** AFM images of solution with 300 ppm Si ion concentration on mica substrate: (a) silica gel seeds (bright spots) as large as 10 nm in diameter appeared after 8 days; (b) network of silica gel developed after 15 days

the actual experiment. For the experiment in solution with 500 ppm Si ion concentration after 10 days of ageing, that value was 0.235g, or equivalent to 2305  $\mu\text{N}$ . Thus 2305  $\mu\text{N}$  is an estimate of the intergranular forces from the silica polymer chains between the two cubes.

SEM images taken of the cubes in solution with 500 ppm Si ion concentration after 10 days of compression in the indenter-puller device showed substantial silica deposits growing around damaged sites, concentrated at one corner of the cube. Not only was the silica gel structure growing on the cube surface around the contact region, it was seen to bridge over microcracks at multiple sites (Fig. 10). In the

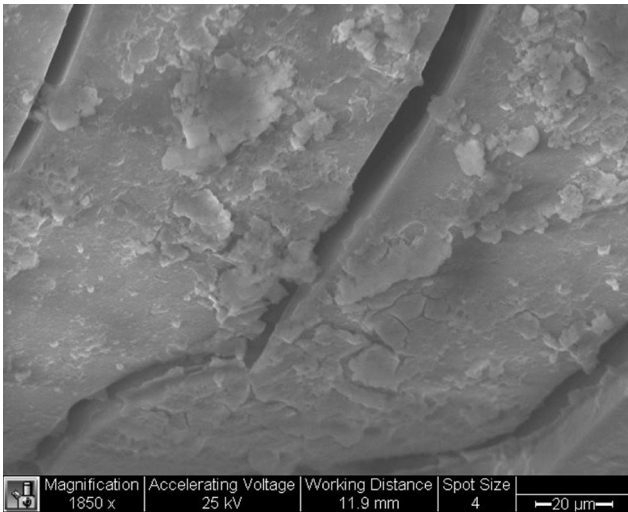


**Fig. 10.** SEM image of cube in cube indenter-puller for 10 days, submerged in 500 ppm Si ion concentration and under 180 N force, after pulling experiment conducted. Three microcracks visible, with extensive silica gel growth on cube surface

figure, three microcracks with width less than  $10\ \mu\text{m}$  are visible. Dehydrated hydrogel structures are indicated the covering cube surface, and other gel structures joining the three microcracks are also marked. Not much of such a deposit was observed on other parts of the cube, where no cracks were present.

For the experiment in solution with 300 ppm Si ion concentration, after 20 days of ageing, extensive silica gel was found between the silica cube debris and the mica sheet (Fig. 11). The massive gel had covered the mica surface near the stressed contact region. It can be clearly seen that the silica cube debris was attached to the mica sheet by the growth of silica gel.

#### *Growth of silica gel in stressed contact region between silica cubes and muscovite mica sheet*

Two silica cubes,  $1.5\ \text{mm} \times 1.5\ \text{mm} \times 1\ \text{mm}$ , were compressed in the pneumatic quartz cube indenter in 300 ppm Si ion concentration solution for 2 weeks with a layer of  $10\ \mu\text{m}$

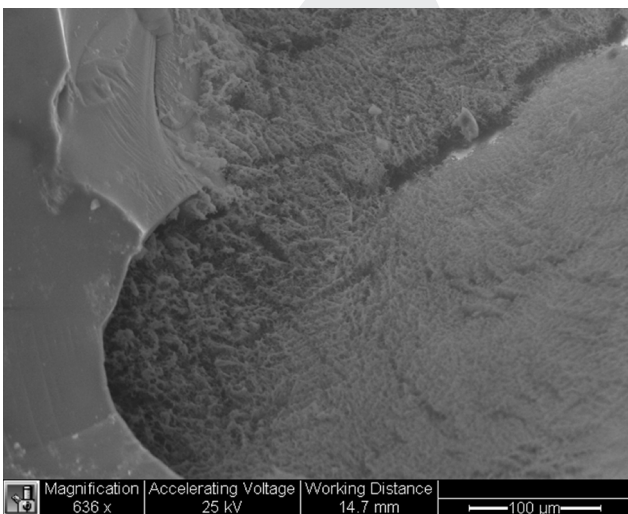


**Fig. 11.** SEM image of silica gel growth on mica sheet near silica cube contact region after 20 days of ageing in 300 ppm Si ion concentration solution. Piece of silica cube debris from contact region adhered to mica sheet by presence of silica gel

muscovite mica sheet between them. SEM images have shown plenty of polymers growing in the vicinity of the contact region on the mica sheet, as well as between the mica sheet and the silica cubes, even though there was no damage on either silica cube (Fig. 12). It can be seen clearly from the image that silica polymers as long as  $100\ \mu\text{m}$  were growing only near the contact region between the silica cube and the muscovite mica sheet, with several polymers having roots on both the cube and the mica. Further away from the contact region, however, no polymers were seen growing on the mica sheet.

#### DISCUSSION AND CONCLUSION

EDS analysis of the polymers found growing between compressed silica cubes in 500 ppm Si ion concentration solution has confirmed that they were indeed made of silica. Traces of chromium and iron may come from the stainless steel chamber in the background. Sodium, nitrogen and chlorine elements may come from the sodium hydroxide and nitric acid used for pH control. If the polymers were of biological origin, carbon would be a major element, but only minor traces of carbon were found.

In the cube-in-compression experiment in 500 ppm Si ion concentration solution, polymers a few hundred micrometres in length were found near the contact region. It can be seen in Fig. 3(a) that the silica polymers in the contact region adhere to both the left and right silica cubes. Such a configuration would create adhesion between the silica cubes at the microscopic level that would enhance the macroscopic strength of sand. In the experiment using the same set-up, but in 300 ppm Si ion concentration solution, deposits of silica gel were found in the cracks. Such deposits were roughly one magnitude smaller than those found at 500 ppm Si ion concentration.

To determine how much effect the stressed contact region has on the precipitation and polymerisation of silica, two types of approach were taken. In the first approach, the experiment was repeated but with a force exerted that was high enough to bring the two cubes in contact, but low enough to prevent any damage to the cubes. No cracks were found on either cube after 3 weeks, and no silica gel deposits were observable anywhere on the cube surfaces. In

2

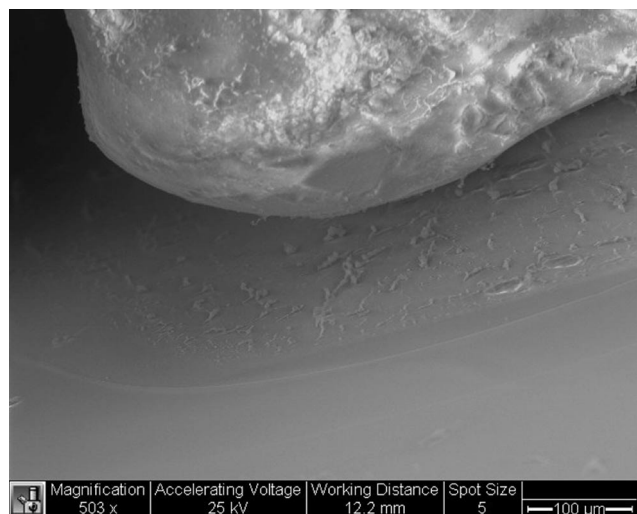


**Fig. 12.** SEM image of stressed contact region between muscovite mica sheet (bottom) and silica cube (top) in 300 ppm Si ion concentration solution under 120 kPa pressure after 2 weeks. Silica polymers growth observed between mica sheet and silica cube in form of filaments between solids in clearly defined region around contact area

the second approach, some 300 ppm Si ion concentration solution was stored separately, undisturbed, and imaged 1 week and 2 weeks later. AFM tapping-mode imaging of the solutions confirmed that, while silica was precipitated and gel structures formed in the solution, their sizes were much smaller than those found in the contact region between stressed silica cubes. Therefore a higher rate of silica precipitation and polymerisation in the liquid chamber around the stressed contact region is detected to have occurred than in the undisturbed solution.

AFM pulling experiments conducted on silica cube surfaces submerged in 210 ppm Si ion concentration for 15 days have shown distinctive, step-like patterns, attributed to silica polymers growing on the cube surfaces. The vertical displacement at each peak, multiplied by the spring constant of the AFM cantilever, yields the average force required to break a single silica polymer chain at 0.39  $\mu\text{N}$ .

The data collected from the indenter-puller showed that the gel structures found between the two silica cubes and the mica sheet contributed an equivalent of 2000  $\mu\text{N}$  force before they were broken when the upper cube was slowly pulled away from the lower cube. These data are the first in the literature to record the magnitude of the force present between silica grains due to intergranular polymers. Even though this force is larger, by four orders of magnitude, than the tensile failure force of a single silica polymer measured in the AFM pulling experiment described above, such a difference is expected, because it represents the force required to break large silica gels composed of a large number of interwoven silica chains.

The solubility of silica at 25°C and neutral pH is 116 ppm (Rimstidt, 1997), but it is thought that the water layer on the surface of silica grain asperities may contain supersaturated silica ions dissolved due to stress. Some of the Si ions may be transported to regions with a lower silica ion concentration, but some of the ions may precipitate near the contact regions and allow the polymerisation process to occur. Although it is still clear how or what quantity of silica is dissolved in saturated solution, the laboratory findings have indicated that silica cubes brought together under compression can accelerate silica precipitation and polymerisation processes, and produce gels that are attached to silica cubes.

Other recent studies have shown that the rate of silica dissolution and precipitation is accelerated in the presence of muscovite mica (e.g. Meyer *et al.*, 2006). The laboratory results confirm such a phenomenon. When two silica cubes were compressed in 300 ppm Si ion concentration solution for 2 weeks without a sheet of mica between them, no polymers were seen anywhere in the liquid chamber when no cracks were initiated in the cubes. When the same experiment was conducted with a muscovite mica layer inserted between the cubes, numerous polymer structures were observed in the contact region on the mica sheet, on the silica cubes, and within the cracks.

Another interesting observation made during the 300 ppm indentation experiment with mica was that all the polymers seen under SEM were in the vicinity of the stressed contact region. Further away from the contact region, no polymers were seen. Such a phenomenon may be due to accelerated dissolution of silica of unobserved microcracks in nearby contact regions and subsequent precipitation from higher silica concentration potential. It indicates the important role of the stressed contact in the dissolution, precipitation and polymerisation of silica.

The results presented are only preliminary. However, they are very important, because for the first time we have a chain of observations that confirms a long-existing hypothesis that a stressed contact with microcracks generates dissolved silica in the contact (asperity) vicinity, which

eventually polymerises, forming a structure between the grain that is sufficiently strong to represent a significant increase of strength, either tensile or eventually, through a rotational deformational mode, also compressive, within a period of time that is of the order of weeks. One of the most important findings is that the failure pulling force of a single chain of the polymer is 330–450 nN. At the grain scale, the failure force of the intergranular bond was found to be 2 mN. Multiple interwoven polymer chains are contained in a single intergranular polymer bond. Notably, such a force is 2.5–10 times higher than the typical capillary force between two spherical grains (8 mm in diameter) at contact failure, being of the order of 0.2–0.8 mN (Mielniczuk *et al.*, 2012). An experimental parametric study is under way to determine the range of validity of the presented findings over different durations of the contact.

#### ACKNOWLEDGEMENTS

The authors acknowledge the support of US NSF grant no. 0700294 of the Civil, Mechanical and Manufacturing Innovation Division, Geomechanics and Geomaterials Program, and in part of a grant from ENI Spa, Milan, Italy.

#### REFERENCES

- Baxter, C. D. P. & Mitchell, J. K. (2004). Experimental study on the aging of sands. *J. Geotech. Geoenviron. Engng* **130**, No. 10, 1051–1062.
- Becker, A. (1995). Quartz pressure solution: influence of crystallographic orientation. *J. Struct. Geol.* **17**, No. 10, 1395–1405.
- Bjorkum, P. (1996). How important is pressure in causing dissolution of quartz in sandstones? *J. Sediment. Res.* **66**, No. 1, 147–154.
- Bowman, E. T. & Soga, K. (2003). Creep, ageing and microstructural change in dense granular materials. *Soils Found.* **43**, No. 4, 107–117.
- Denisov, N. Y. & Reltov, B. F. (1961). The influence of certain processes on the strength of soils. *Proc. 5th Int. Conf. Soil Mech. Found. Engng, Paris* **1**, 75–78.
- Eyring, H. (1936). Viscosity, plasticity, and diffusion as examples of absolute reaction rates. *J. Chem. Phys.* **4**, No. 4, 283–291.
- Heald, M. T. (1955). Stylolites in sandstones. *J. Geol.* **63**, No. 2, 101–114.
- Hickman, S. & Evans, B. (1995). Kinetics of pressure solution at halite-silica interfaces and intergranular clay films. *J. Geophys. Res.* **100**, No. B7, 13113–13132.
- Hu, L. B. & Hueckel, T. (2007a). Coupled chemo-mechanics of intergranular contact: toward a three-scale model. *Comput. Geotech.* **34**, No. 4, 306–327.
- Hu, L. B. & Hueckel, T. (2007b). Creep of saturated materials as a chemically enhanced rate-dependent damage process. *Int. J. Numer. Anal. Methods Geomech.* **31**, No. 14, 1537–1565.
- Hueckel, T., Cassiani, G., Tao, F. & Pellegrino, A. (2001). Aging of oil/gas-bearing sediments, their compressibility, and subsidence. *J. Geotech. Geoenviron. Engng* **127**, No. 11, 926–938.
- Hueckel, T., Cassiani, G., Prévost, J. H. & Walters, D. A. (2005). Field derived compressibility of deep sediments of the Northern Adriatic. *Proc. 7th Int. Symp. on Land Subsidence, Shanghai*, 35–49.
- Iler, R. K. (1955). The colloid chemistry of silica and silicates. *Soil Sci.* **80**, No. 1, 86.
- Israelachvili, J. N. (2011). *Intermolecular and surface forces*, 3rd edn. Burlington, MA: Academic Press.
- Joshi, R. C., Achari, G., Kaniraj, S. R. & Wijeweera, H. (1995). Effect of aging on the penetration resistance of sands. *Can. Geotech. J.* **32**, No. 5, 767–782.
- Kristiansen, K., Valtiner, M., Greene, G. W., Boles, J. R. & Israelachvili, J. N. (2011). Pressure solution: the importance of the electrochemical surface potentials. *Geochim. Cosmochim. Acta* **75**, No. 22, 6882–6892.
- Kuhn, M. R. & Mitchell, J. K. (1993). New perspectives on soil-creep. *J. Geotech. Engng ASCE* **119**, No. 3, 507–524.

- Mesri, G., Feng, T. & Benak, J. (1990). Postdensification penetration resistance of clean sands. *J. Geotech. Engng ASCE* **116**, No. 7, 1095–1115.
- Meyer, E. E., Greene, G. W., Alcantar, N. A., Israelchvili, J. N. & Boles, J. R. (2006). Experimental investigation of the dissolution of quartz by a muscovite mica surface: implications for pressure solution. *J. Geophys. Res. Solid Earth* **111**, No. B08202, <http://dx.doi.org/10.1029/2005JB004010>.
- Mielniczuk, B., Hueckel, T., *et al.* (2012). Evolution due to evaporation of capillary bridges between two spheres: experiments. *Phys. Rev. E* (submitted).
- Mitchell, J. K. & Solymar, Z. V. (1984). Time-dependent strength gain in freshly deposited or densified sand. *J. Geotech. Engng ASCE* **110**, No. 11, 1559–1576.
- Oelkers, E. H., Bjorkum, P. A. & Murphy, W. M. (1992). The mechanism of porosity reduction, stylolite development and quartz cementation in North Sea sandstones. *Proc. 7th Int. Symp. on Water-rock Interaction, Park City, UT*, 1183–1186.
- Oelkers, E. H., Schott, J., Gauthier, J.-M. & Herrero-Roncal, T. (2008). An experimental study of the dissolution mechanism and rates of muscovite. *Geochim. Cosmochim. Acta* **72**, No. 20, 4948–4961.
- Parry, R. H. G. (2004). *Mohr circles, stress paths and geotechnics*, 2nd edn. London: Spon Press.
- Paterson, M. S. & Kekulawala, K. (1979). Role of water in quartz deformation. *Bull. Mineralog.* **102**, No. 2–3, 92–98.
- Renard, F., Ortoleva, P. & Gratier, J. P. (1997). Pressure solution in sandstones: influence of clays and dependence on temperature and stress. *Tectonophysics* **280**, No. 3–4, 257–266.
- Rimstidt, J. D. (1997). Quartz solubility at low temperatures. *Geochim. Cosmochim. Acta* **61**, No. 13, 2553–2558.
- Rubin, C. J. (2009). *A novel apparatus for the study of intergranular silica microstructures*. Durham, NC: Duke University.
- Rutter, E. H. (1976). Kinetics of rock deformation by pressure solution. *Phil. Trans. R. Soc. London Ser. A* **283**, No. 1312, 203–219.
- Schmertmann, J. H. (1991). The mechanical aging of soils. *J. Geotech. Engng ASCE* **117**, No. 9, 1288–1330.
- Scholz, C. H. & Engelder, J. T. (1976). Role of asperity indentation and plowing in rock friction. 1. Asperity creep and stick-slip. *Int. J. Rock Mech. Mining Sci.* **13**, No. 5, 149–154.
- Sorby, H. C. (1862). The Bakerian Lecture: On the direct correlation of mechanical and chemical forces. *Proc. R. Soc. London* **12**, 538–550.
- Tada, R., Maliva, R. & Siever, R. (1987). A new mechanism for pressure solution in porous quartzose sandstone. *Geochim. Cosmochim. Acta* **51**, No. 9, 2295–2301.
- Wang, Y. H. & Tsui, K. Y. (2009). Experimental characterization of dynamic property changes in aged sands. *J. Geotech. Geoenviron. Engng ASCE* **135**, No. 2, 259–270.
- Wang, Y. H., Xu, D. & Tsui, K. (2008). Discrete element modeling of contact creep and aging in sand. *J. Geotech. Geoenviron. Engng ASCE* **134**, No. 9, 1407–1411.
- Worden, R. H. & Morad, S. (2000). Quartz cementation in oil field sandstones: a review of the key controversies. In *Quartz cementation in sandstones* (eds R. H. Worden and S. Morad), Special Publication 29, International Association of Sedimentologists, pp. 1–20. Malden, MA: Blackwell Science.

4

- 1: Figure 8 is in black & white, not colour. Which curve is which (i.e. upper and lower rather than red and blue)?
- 2: This reference doesn't seem to be correct. What should the correct reference be?
- 3: I've added missing bibliographic information (e.g. page numbers, co-authors; names). Please check carefully.
- 4: Please provide names of all authors. Has this now been accepted for publication? If not, is it valid to cite as a reference?
- 5: Please note that I've deleted the rest of this caption, as it merely duplicates the text.